Electronic relaxation of alkali metal atoms on the Cu(111) surface

ARTICLE *in* SURFACE SCIENCE · APRIL 2000

Impact Factor: 1.93 · DOI: 10.1016/S0039-6028(00)00004-2

ELSEVIER

Surface Science 451 (2000) 22–30

surface science

www.elsevier.nl/locate/susc

Electronic relaxation of alkali metal atoms on the Cu(111) surface

H. Petek *, M.J. Weida, H. Nagano, S. Ogawa

Advanced Research Lab., Hitachi, Ltd, Hatoyama, Saitama 350-0395, Japan

Received 24 August 1999; accepted for publication 13 October 1999

Abstract

Interferometric time-resolved two-photon photoemission measurements are performed on Cs and Rb chemisorbed on Cu(111). The population decay of the alkali-atom-induced anti-bonding state at 35 K is observed on 50 fs and 20 fs time scales for Cs and Rb respectively. Factors that contribute to such unusually long lifetimes, and in general determine the lifetimes of adsorbates on metal surfaces, are discussed in light of related measurements by Bauer et al. [Phys. Rev. B 60 (1999) 5016] and theoretical simulations by Borisov et al. [Surf. Sci. 430 (1999) 165].

Keywords: Alkali metals; Chemisorption; Copper; Photon photoemission

1. Introduction

The rate of electronic relaxation of atoms and molecules at distances of a few angstroms above a metal surface is the controlling factor in a variety of phenomena, including surface photochemistry, desorption induced by electronic transitions, scattering of energetic particles from surfaces, etc. [1,2]. Until recently, lifetimes of the electronically excited adsorbates could only be estimated from indirect measurements, such as photodesorption quantum yields, or linewidths of resonances observed through a variety of spectroscopic techniques, such as electron energy loss spectroscopy, inverse photoemission [3,4], and two-photon photoemission (2PP) [5,6]. These indirect methods imply universally short lifetimes of $\ll 10$ fs due to essentially unhindered flow of energy or charge into the metal bulk. Homogeneous spectral linewidths include information on all dynamical processes that lead to the decay of the quantum mechanical phase. However, for solid state materials, linewidths provide only a lower limit for the excited state lifetime through the Heisenberg uncertainty relation $\Gamma\tau \geq \hbar$ [7]. This is due to unavoidable contributions to the linewidth from quasi-elastic processes such as the electron–phonon (e–p) scattering and inhomogeneities due to disorder, impurities, or band dispersion, which are difficult to disentangle from the population decay [8–11].

Lifetimes of excited states at metal surfaces can be studied much more directly in the time domain by techniques such as time-resolved two-photon photoemission (TR-2PP) [6]. State-of-the-art femtosecond lasers provide sufficient time resolution to probe the dynamics of intrinsic and adsorbate

* Corresponding author. Fax: +81-492-966006.
E-mail address: petek@harl.hitachi.co.jp (H. Petek)

0039-6028/00/$ - see front matter
PII: S0039-6028(00)00004-2

modified image potential (IP) states on metal surfaces. IP states at the metal–vacuum interface are sufficiently decoupled from the bulk to allow direct time-domain lifetime measurements on 10–1000 fs time scales [12–15]. The IP state lifetimes are particularly long because projected bandgaps that exist for many metals prevent significant penetration of the electron wavefunctions into the bulk, where ultrafast population decay occurs through electron–electron (e–e) scattering. Although only a few time-resolved measurements are reported for adsorbate-induced states on metal surfaces, the results for most part confirm the expectations from linewidth analysis and photodesorption quantum yields. For instance, Wolf and coworkers report the upper limit for the lifetime of the CO $2\pi^*$ state on Cu(111) at $\sim$3.5 eV above E_F of $<$5 fs, which is consistent with a lower limit of $>$1 fs from the 2PP linewidth analysis [16,17], and the extremely small quantum yields for the electron stimulated desorption of CO. However, the unusually long lifetimes of alkali metal atoms on noble metal surfaces found by Bauer and coworkers [18–20] provide a counter example showing that electronically excited adsorbates can persist on metal surfaces for $>$50 fs [21–23], which is at least an order of magnitude longer than anticipated from indirect estimates for other systems.

It is the purpose of this paper to review briefly the previous work on the electronically excited alkali metal atom lifetimes on metal surfaces, with a particular emphasis on the interferometric time-resolved two-photon photoemission (ITR-2PP) measurements on Cs–Cu(111), and to compare them with the new results on Rb–Cu(111). Significant differences in lifetimes for different substrates and adsorbates provide a basis for discussion of various subtle factors that may affect the electronic relaxation rates of adsorbate localized excitations at metal surfaces.

2. Alkali metal atom chemisorption

The investigation of chemisorption of the alkali metal atoms on metal surfaces has a long history, dating to the pioneering studies of Langmuir. Despite more than 70 years of intensive investigation, a consistent picture of the alkali metal atom chemisorption that can fully explain its various facets is still elusive. According to the Langmuir–Gurney (LG) model for the alkali metal chemisorption [24,25], the *n*s valence electron of an alkali metal atom approaching a metal surface experiences repulsion from the positive core-induced image charge in the metal [25,26]. Beyond a distance where the *n*s orbital crosses above the Fermi level E_F resonant charge transfer (RCT) can occur into the unoccupied states of the metal. At the chemisorption distance the *n*s orbital is shifted several electron-volts above E_F due to the Coulomb repulsion, and extremely fast tunneling between the alkali metal atom and the surface induces a large bandwidth, as shown in Fig. 1a [25,26,28]. According to the LG model, in the low alkali metal coverage limit the alkali metal atoms are nearly fully ionized since only a small fraction

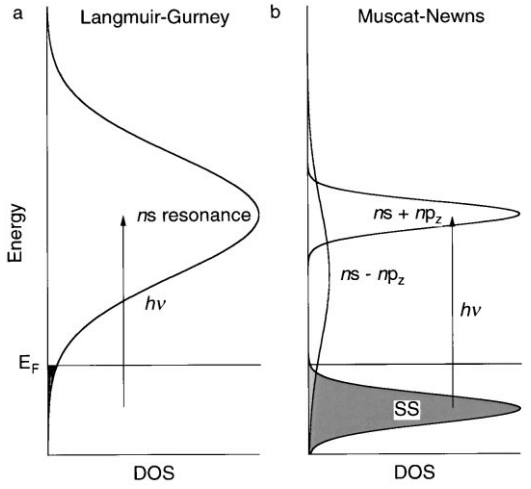

Fig. 1. Two models for the chemisorption of alkali metal atoms on metals and photoexcitation to the unoccupied resonance. (a) According to the LG model the unoccupied state corresponds to the alkali atom *n*s resonance, which is shifted above E_F and broadened by the interaction with the metal. Photoexcitation can occur by intraband transition from the occupied to the unoccupied density of states [24,25]. (b) According to the Muscat–Newns model the *n*s and *n*p orbitals of the alkali atom hybridize into $ns-np_z$ bonding and $ns+np_z$ anti-bonding orbitals [18,27]. The former is not observed due to its large bandwidth, but it contributes to the transition moment through the hybridization with the occupied Shockley surface state, SS. The photoexcitation occurs by interband transition from SS to the $ns+np_z$ anti-bonding state.

of the total *n*s density is occupied. The alkali metal atoms form a disordered layer due to strong depolarization field-induced repulsion; however, as the coverage increases to a monolayer thickness the alkali metal film becomes metallic, implying increased occupation of the *n*s band. Though this description is intuitively appealing, it fails to explain many experimental aspects of the alkali metal atom chemisorption, such as the lack of coverage dependence of the alkali metal atom–substrate bond length due to the ionic-to-metallic transition, or the preference of the large alkali metal atoms (K, Rb, and Cs) for adsorption at the atop sites on close-packed surfaces [29]. The density functional calculations of Ishida and Liebsch challenge the LG model by showing that even at low coverage the *n*s electron is mainly localized between the alkali metal and the substrate, implying that the bond has covalent character [30,31]. According to Muscat and Newns (MN), intra-atomic hybridization of alkali metal atom *n*s and np_z orbitals near a metal surface may result in a pair of $ns-np_z$ and $ns+np_z$ bonding and anti-bonding orbitals where the electron density is either localized between the alkali metal atom and the substrate or is projecting into the vacuum [27,32], as shown in Fig. 1b. In principle, studies of the electronic structure should be able to distinguish between the two descriptions in Fig. 1. However, the density of states associated with the bonding interaction has not been firmly established by the gamut of electronic spectroscopy techniques [33–35]. Nevertheless, a ubiquitous feature of the electronic structure of alkali metal atoms on a variety of metal surfaces at low coverage is an unoccupied state at ~ 3 eV above E_F found in inverse photoemission [3,4] and 2PP spectra [18,19,36]. The MN model is preferred because the narrow linewidth of this unoccupied state (e.g. <70 meV for Cs–Cu(111) at ~ 2.5 eV [21]) is incompatible with the predictions of >0.8 eV for the bonding state [27,28,32]. Such large width implies complete ionization of Cs atoms, which is inconsistent with the chemisorption bond lengths [29]. The direct time-domain measurement of the lifetime of the anti-bonding state for Cs–Cu(111) and Rb–Cu(111) is the subject of this paper.

3. Experimental

The ITR-2PP experiment and data evaluation method are described in more detail elsewhere [6]. Briefly, frequency-doubled light from a Ti:sapphire laser ($h\nu = 3.08$ eV; 13 fs intensity pulse width) is split into equal pump and probe pulses in a feedback-controlled scanning Mach–Zehnder interferometer. The pump–probe delay is scanned by ± 150 fs with an accuracy of $<\lambda/25$ corresponding to 5×10^{-17} s for repetitive scans. The pulses are focused collinearly to a spot of 80 μm on the sample, which is held in an ultrahigh vacuum (UHV) chamber (base pressure: $<5\times10^{-11}$Torr). p-Polarized light incident at 30° from the surface normal excites 2PP, which is measured as a function of energy at $k_{\parallel}=0$ with a hemispherical electron energy analyzer (5° angular, and <30 meV energy resolution). 2PP spectra are measured with single pulse excitation by scanning the analyzer pass energy. Electronic relaxation rates are obtained from interferometric two-pulse correlation (I2PC) measurements, where the 2PP current is monitored at a specific energy as a function of the pump–probe delay. The Cu(111) surface is cleaned by a cyclic procedure of Ar^+ sputtering (500 V) and annealing at 700 K. The sample temperature is set between 33 and 300 K by a He closed-cycle refrigerator–heater combination. Cs and Rb are evaporated onto a room temperature Cu(111) surface from an SAES getter while maintaining the UHV chamber pressure in the 10^{-10} Torr range. The change in the work function Φ, as determined by 2PP spectra, is used to determine the Cs coverage from a literature calibration curve [37]. The same curve also provides a first-order estimate of the Rb coverage.

4. Results

A clean Cu(111) surface has a projected band gap extending between the $L_{2'}$ and L_1 points at -0.85 and 4.08 eV, which supports a Shockley-type surface state (SS) with an energy of -0.39 eV for $k_{\parallel}=0$ [15]. When Cs is deposited on the Cu(111) surface a new unoccupied state at 3.1 eV (the low coverage limit) can be observed by 2PP

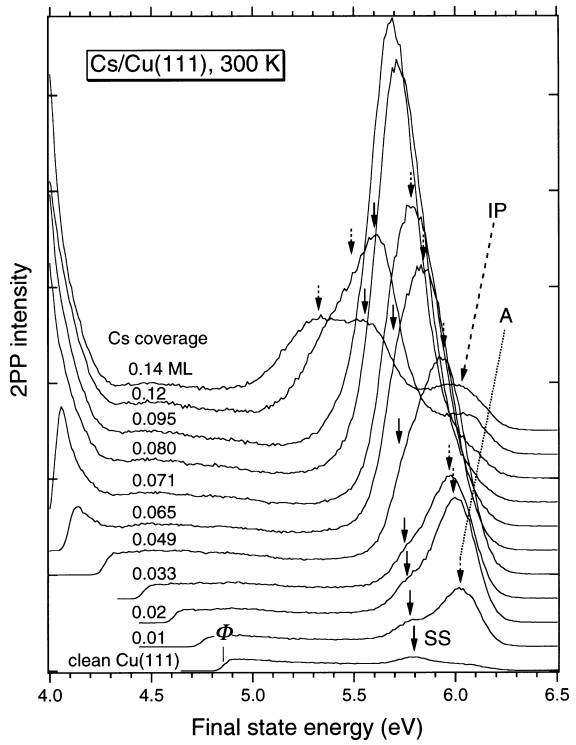

Fig. 2. 2PP spectra of Cs–Cu(111) for different Cs coverages. For a clean surface the only peak is due to two-photon absorption from SS (position indicated by full arrow). Upon chemisorption of Cs the work function Φ decreases and a new feature due to the anti-bonding state A appears (position indicated by dotted arrow). Since both the energy of Φ and A strongly depend on the Cs coverage it is possible to achieve resonant SS→A excitation with 3.1 eV photons for ~0.095 ML of Cs. At the highest coverages an extra peak due to the IP states appears (position indicated by dashed arrow).

[3,18]. This state will be referred to as the anti-bonding state A. An increase in Cs coverage results in a characteristic decrease in Φ changing the shape of the image potential. As a result the energies of A, and to a lesser extent SS, also decrease [18,36,37]. Therefore, direct SS→A excitation with 3.1 eV light is possible by tuning the transition energy into resonance with the excitation light by means of the Cs coverage, as shown in Fig. 2. Resonance enhancement is clearly seen, since the intensity of the main peak for a coverage of ~0.10 ML is larger than the sum of individual SS and A peak intensities for nonresonant excitation conditions. Bauer et al. [20] do not find this enhancement, and therefore attribute the excitation of A to a transition from the bulk bands of Cu(111) [3,20]. Though the reason for this is not understood, it may be related to a different angle of incidence of the excitation light (45°) in their experiment. Although the spatial overlap between A and SS is poor, since the former is localized and the latter is not, the transition moment may be enhanced by the interaction between the $ns-np_z$ hybridized bonding orbital of Cs and SS, as implied in Fig. 1. Whether the alkali metal atom–surface bond at low coverage is assumed to be ionic or covalent, photoexcitation results in a large charge redistribution that can be regarded either as back electron transfer or as redistribution of charge from the alkali metal atom–substrate bond towards the vacuum respectively.

The lifetime of the anti-bonding state is investigated by ITR-2PP. Fig. 3 shows a 2PP spectrum for near resonant SS→A excitation and phase-averaged I2PC measurements at 33 K for several energies across this resonance. In the I2PC scans of Fig. 3b the dependence of the 2PP signal intensity on the delay between identical pump and probe pulses provides information on the population dynamics of A and the coherence between the optically coupled levels. Although the measurement is performed with interferometric scanning, the interference fringes resulting from the coherence in the excitation process are suppressed by averaging the I2PC signal over the optical phase in order to emphasize just the population dynamics [21,23]. More detailed discussion of the coherence can be found in Refs. [21–23]. The signal consists of a coherent spike, which decays within ~30 fs, and a longer *nonexponential* decay that is observed for delays of up to ~150 fs. The latter component provides information on the population dynamics of A, which are complex because the electronic excitation 'turns on' the repulsive interaction between Cs and Cu. The decays are nonexponential because the ensuing nuclear motion of Cs atoms can affect the surface electronic structure, the lifetime, and the transition moment for photoemission [38]. Thus, the observed decays have a peculiar time-dependence because of the stretching of the Cu–Cs bond length R_{Cu-Cs}. Nuclear motion along the dissociation coordinate may be antici-

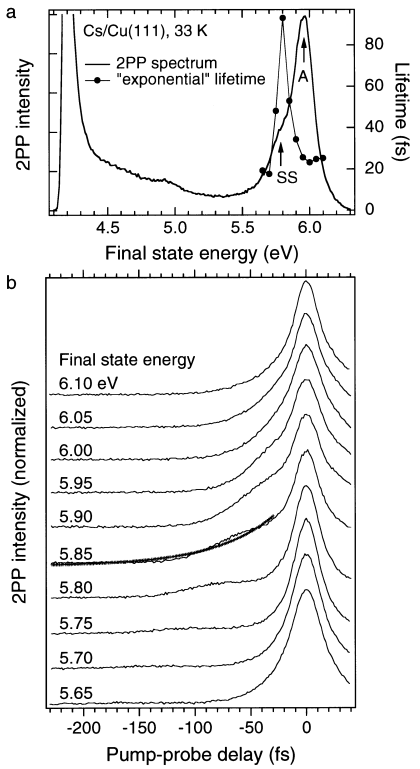

Fig. 3. (a) 2PP spectrum of Cs–Cu(111) for a coverage of ~0.08 ML and the effective lifetimes of the antibonding state. Arrows indicate the contributions from SS and A to the 2PP spectrum. (b) Phase-averaged I2PC scans near the SS→A resonance. Calculated exponential decay corresponding to a lifetime of 50 fs is indicated for the final state energy of 5.85 eV.

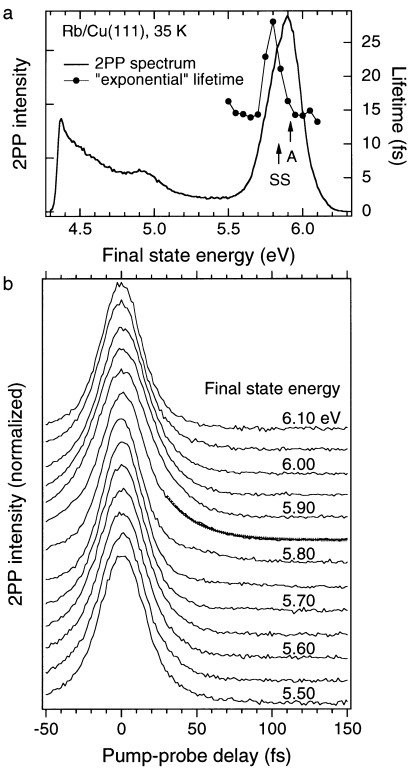

Fig. 4. (a) 2PP spectrum of Rb–Cu(111) for a coverage of ~0.05 ML and the effective lifetimes of the antibonding state. Arrows indicate the contributions from SS and A to the 2PP spectrum. (b) Phase-averaged I2PC scans near the SS→A resonance, which show a longer decay near the SS→A resonance. Calculated exponential decay corresponding to a lifetime of 22 fs is indicated for the final state energy of 5.85 eV.

pated from the observation of photodesorption of K from graphite [39]. Even though the decays are nonexponential, a rough estimate of ~50 fs at 0.1 eV below the energy of A can be obtained by forcing an exponential fit, as shown in Fig. 3. The decay is significantly faster at higher temperatures, which is in agreement with a ~15 fs lifetime at 300 K reported by Bauer et al. [20], as discussed previously [21]. Since this is an extraordinarily long lifetime for a metal–adsorbate system, it is worthwhile to search for general trends that may inhibit electronic quenching in Cs–Cu(111).

With this in mind, Fig. 4 presents the 2PP spectra and phase averaged I2PC measurements for Rb–Cu(111) under near resonant SS→A excitation conditions as for Cs–Cu(111) in Fig. 3. Rubidium has similar chemisorption properties on metals to cesium, so it is likely to exhibit analogous excited state dynamics [29]. In the case of Rb–Cu(111) the I2PC amplitudes decay much faster than for Cs–Cu(111); however, there is still a noticeable broadening of the traces near the SS→A resonance corresponding to a 'lifetime' of ~20 fs. Again, the decay of signal from A is nonexponential, but to a lesser degree than for Cs. The lifetime of A does not allow for significant nuclear motion of the Rb atoms, and, therefore, the signal is probably dominated by the electronic relaxation. The comparison between Rb and Cs chemisorption systems shows that although the decay of the anti-bonding state on Cs–Cu(111) is unusually slow, similar trends can be observed for smaller alkali metal atoms such as Rb on Cu(111). By

contrast, in corresponding measurements (not shown) on Cs–Cu(100) and Cs–Cu(110) the lifetime of the anti-bonding state is the same as for the bulk hot electrons at the same energy, indicating that the electronic excitation is rapidly delocalized into the metal [40].

5. Discussion

The measurements in Section 4 show a trend for a longer lifetime of A on Cu(111) for larger and more polarizable alkali metal atoms. Other measurements also point to a strong influence of the crystalline orientation and composition of the substrate [20,40]. Bauer et al. report results on several other related alkali metal chemisorption systems at 300 K [18,19]. Their $\sim$15 fs lifetime of A for Cs–Cu(111) is consistent with the present measurements since the lifetime rapidly decreases at higher temperature, as described in detail in Ref. [21]. However, they also report a lifetime of $\sim$6 fs for Cs–Cu(100) at 300 K, which could not be reproduced here with higher temporal resolution and sensitivity at 50 or 300 K [22]. The reason for this discrepancy is not understood. Bauer et al. [20] also report a tentative lifetime of $>$7 fs for Cs–Ag(111), whereas for Na–Cu(100) it is too fast to measure. Thus the unusually long lifetimes of A for Cs–Cu(111) appear to reflect special properties of both adsorbate and the substrate.

Several factors in combination, such as the $ns+np_z$ anti-bonding hybridization, the *L*-projected band gap for Cu(111), and atop chemisorption site appear to be responsible for these trends. Bauer et al. [18,19,41] argue that the hybridization of A and the large size of Cs atoms displaces the electron density into the vacuum resulting in a poor overlap with the bulk bands of the metal [27]. The argument regarding the hybridization is supported by theory [31,38]. Borisov et al. [42] calculate that for Cs–Cu(111) the electronic cloud density maximum is displaced by 0.9–1.1 Å from the Cs atom into the vacuum. According to unpublished LEED measurements, the Cs and Cu atoms that form the bond are 3.09 Å above and 0.12 Å below the Cu atom plane [43]. Thus the charge density of A is displaced by $\sim$4 Å into the vacuum, which is comparable or even larger than the calculated density maximum for the $n=1$ IP state for Cu(111), which has a lifetime of 22 fs at 25 K [15,44]. The argument regarding the size and bond length is less convincing. Borisov et al. [42] calculate that the lifetime of A on average *increases* as the Cs atom distance from the Cu atom plane decreases from 4.3 to 2.8 Å. This is contrary to what is expected for a jellium surface [26], and is specifically attributable to the projected band gap. Also, the measurements for Rb–Cu(111) do not provide support for significant alkali metal atom size dependence. Both ionic and covalent radii, which are smaller by $\sim$0.2 Å for Rb, suggest that R_{Cu-Rb} is $\sim$10% shorter than R_{Cu-Cs}. This could lead to a significant enhancement in relaxation. However, since the actual bond length $R_{Cu-Rb}=3.07$ Å is comparable to R_{Cu-Cs} [45], and the calculated relaxation rate of Cs *decreases* at the distance corresponding to R_{Cu-Rb} [42], the size of the alkali metal atom may not explain the difference between Rb and Cs. A more likely explanation for the Cs and Rb results is the difference in their atomic polarizability [27]. Differences in the energies of the *n*s and *n*p orbitals of 1.39 eV versus 1.56 eV and static polarizabilities of 53 Å^3 versus 40 Å^3, for free Cs and Rb atoms respectively, imply a different degree of polarization of the charge density away form the surface [27,46]. Thus the degree of hybridization-induced charge redistribution may be the key to understanding the alkali metal atom dependence of the lifetime of A.

Both Ogawa et al. [21] and Borisov et al. [42] conjecture that the unusually long lifetimes on the Cu(111) surface are due to the localization of A in the *L*-projected band gap, but for qualitatively different reasons. 2PP studies of IP states firmly establish that 2D delocalized surface states in band gaps have considerably longer lifetimes than surface resonances, which are degenerate with bulk bands of the same parallel momentum [14,15,47]. The existence within a band gap restricts the IP state wavefunctions to the solid–vacuum interface, where the e–e scattering is less efficient than in the

bulk. However, it is not clear whether momentum conservation imposes similar constraints on the coupling of disordered chemisorbates, where momentum is not defined, with isoenergetic bulk bands. Borisov et al. [42] argue that although coupling to large parallel momentum bulk bands is possible, for decay through the RCT mechanism the rates for $k_{\parallel} \neq 0$ are significantly slower because of a larger tunneling barrier width in off-normal directions. However, this argument fails to explain the exceedingly short lifetime of the $2\pi^*$ state of CO–Cu(111) [17], and it predicts a general trend for larger photodesorption yields on the late period (111) surfaces with *L*-projected band gaps than for the corresponding lower symmetry surfaces, which is not supported in published literature [1,2].

Ogawa et al. [21] argue that the symmetry of interacting orbitals of adsorbates on Cu(111) explains the large differences in the decay rates of the unoccupied states of Cs and CO [48]. For symmetry reasons the 6s and $6p_z$ orbitals of Cs atoms on the atop site can overlap only with the 4s, $4p_z$, $3d_{3z^2-1}$ orbitals of the substrate. However, maximum overlap with these bands can be achieved at $k_{\parallel} = 0$, where the difference in energy between the interacting states is 3 eV. In the hollow sites, which can have significant thermal population at 300 K [21], the symmetry of Cs orbitals allows for the *resonant* interaction with the $4p_x$ and $4p_y$ orbitals of the substrate, which contribute to the Q_2 band in the *L–W* direction. Therefore, alkali metal atoms in the hollow sites may interact with the bulk bands more strongly than in the atop sites. The site dependence of alkali metal atom–metal substrate interaction is consistent with trends in the electronic relaxation of A with temperature, the crystal face of copper, and substrate material.

Further information on the electronic relaxation of alkali metal atoms can be gleaned from the analysis of resonant Auger Raman (RAR) intensities of alkali metal atom-like rare-gas adsorbates on metal surfaces [35,49]. Rare-gas atoms with valence shell occupation of corresponding alkali metal atoms can be prepared at physisorption bond distances by X-ray absorption from the core to a resonance, which is assigned to the *n*s orbital. This resonance appears to be related to the antibonding state appearing in the IP and 2PP spectra; however, it is generally at a lower energy, since the excitation occurs at a physisorption distance, which is generally 10–15% larger than that for the corresponding alkali metal atom chemisorption [35]. The RAR intensities are determined by the loss of coherence in the excitation, and thus can be compared with the homogeneous linewidths of the corresponding states in 2PP. The loss of coherence is attributed to the charge transfer of the *n*s electron to the metal, which is plausible, but it may also have contributions from other processes, such as the e–p interaction, which is considerable for Cs–Cu(111) [21]. The RAR charge transfer rates and 2PP linewidths are consistent, though there are no data on directly related systems for which such a comparison would be most meaningful [20,35]. Sandell et al. [35] conclude that the charge transfer rate decreases as the work function of the metal is increased. This suggests that for an alkali metal atom–metal substrate system the lifetime of A should also depend on the alkali metal coverage (i.e. work function); however, Bauer et al. [20] find that the lifetime of A in Cs–Cu(111) is independent of Φ over a range of 0.8 eV. Clearly further RAR and TR-2PP studies on related systems are necessary to extract complimentary information on the electronic relaxation of alkali metal atoms near metal surfaces.

6. Conclusions

Although the unoccupied band structure of alkali metal atom–metal substrate chemisorption system at low adsorbate coverage shows great similarities for a broad range of adsorbates and substrates, the alkali-metal-atom-induced antibonding state lifetime shows exquisite sensitivity on the nature of the adsorbate and the substrate. Contrasting electronic relaxation rates of Cs and Rb chemisorbed on Cu(111) presented here, as well as measurements on other related systems by Bauer and coworkers [18–20,41], point to several key factors that in combination contribute to the exceptionally slow relaxation rate for Cs–Cu(111). Owing to the large size and polarizability of Cs

the anti-bonding state density appears to be effectively displaced from the Cu—Cs bond to the vacuum side of the alkali metal atom, where the interaction with the surface is weak [42]. In addition, the location of the anti-bonding state in the middle of the *L*-projected band gap combined with an atop adsorption site effectively prevents the delocalization of the excitation into the metal bulk. As result of this confinement of the anti-bonding state at the surface, the relaxation process appears to be dominated by the much smaller electronic density at the surface, as for the IP states [42,50]. Future ITR-2PP studies of the alkali metal atom–metal substrate adsorption system should provide further valuable insights on factors that govern the lifetimes of adsorbates on metal surfaces.

Acknowledgements

The authors thank Y. Matsumoto for valuable discussions regarding photochemistry on metal surfaces, and N. Moriya, N. Matsunami, and S. Saito for technical support. The authors thank New Energy Development Organization for the International Joint Research Grant, which provided partial funding for this project. M.J. Weida wishes to thank the National Science Foundation and the Center for Global Partnership for support (NSF grant INT-9819100).

References

[1] R.R. Cavanagh, D.S. King, J.C. Stephenson, T.F. Heinz, J. Phys. Chem. 97 (1993) 786.
[2] F.M. Zimmermann, W. Ho, Surf. Sci. Rep. 22 (1995) 127.
[3] D.A. Arena, F.G. Curti, R.A. Bartynski, Phys. Rev. B 56 (1997) 15 404.
[4] D. Haskett, K.-H. Frank, K. Horn, E.E. Koch, H.-J. Freund, A. Baddorf, K.-D. Tsuei, E.W. Plummer, Phys. Rev. B 37 (1988) 10 387.
[5] T. Fauster, W. Steinmann, in: P. Halevi (Ed.), Electromagnetic Waves: Recent Developments in Research, vol. 2, Elsevier, Amsterdam, 1994, p. 1.
[6] H. Petek, S. Ogawa, Prog. Surf. Sci. 56 (1997) 239.
[7] H. Petek, H. Nagano, S. Ogawa, Phys. Rev. Lett. 83 (1999) 832.
[8] B.A. McDougall, T. Balasubramanian, E. Jensen, Phys. Rev. B 51 (1995) 13 891.
[9] S.D. Kevan, Phys. Rev. B 33 (1986) 4364.
[10] F. Theilmann, R. Matzdorf, G. Meister, A. Goldmann, Phys. Rev. B 56 (1997) 3632.
[11] C. Reuß, I.L. Shumay, U. Thomann, M. Kutschera, M. Weinelt, T. Fauster, U. Höfer, Phys. Rev. Lett. 82 (1999) 153.
[12] R.W. Schoenlein, J.G. Fujimoto, G.L. Eesley, T.W. Capehart, Phys. Rev. B 41 (1990) 5436.
[13] C.B. Harris, N.-H. Ge, R.L. Lingle, J.D. McNeill, Annu. Rev. Phys. Chem. 48 (1997) 711.
[14] U. Höfer, I.L. Shumay, C. Reuß, U. Thomann, W. Wallauer, T. Fauster, Science 277 (1997) 1480.
[15] E. Knoesel, A. Hotzel, M. Wolf, J. Electron Spectrosc. Relat. Phenom. 88–91 (1998) 577.
[16] E. Knoesel, T. Hertel, M. Wolf, G. Ertl, Chem. Phys. Lett. 249 (1995) 409.
[17] L. Bartels, G. Meyer, K.-H. Rieder, D. Velic, E. Knoesel, A. Hotzel, M. Wolf, G. Ertl, Phys. Rev. Lett. 80 (1998) 2004.
[18] M. Bauer, S. Pawlik, M. Aeschlimann, Phys. Rev. B 55 (1997) 10 040.
[19] M. Bauer, Ph.D. Thesis, Swiss Federal Institute of Technology, Zurich, 1998.
[20] M. Bauer, S. Pawlik, M. Aeschlimann, Phys. Rev. B 60 (1999) 5016.
[21] S. Ogawa, H. Nagano, H. Petek, Phys. Rev. Lett. 82 (1999) 1931.
[22] S. Ogawa, H. Nagano, H. Petek, Appl. Phys. B 68 (1999) 611.
[23] S. Ogawa, H. Nagano, H. Petek, Surf. Sci 427–428 (1999) 34.
[24] I. Langmuir, J. Am. Chem. Soc. 54 (1932) 2798.
[25] R.W. Gurney, Phys. Rev. 47 (1935) 479.
[26] P. Nordlander, J.C. Tully, Phys. Rev. B 42 (1990) 5564.
[27] J.P. Muscat, D.M. Newns, Surf. Sci. 84 (1979) 262.
[28] J.P. Muscat, D.M. Newns, Prog. Surf. Sci. 9 (1978) 1.
[29] R.D. Diehl, R. McGrath, J. Phys. C 9 (1997) 951.
[30] H. Ishida, Phys. Rev. B 38 (1988) 8006.
[31] H. Ishida, A. Liebsch, Phys. Rev. B 45 (1992) 6171.
[32] J.P. Muscat, D.M. Newns, Surf. Sci. 74 (1978) 355.
[33] B. Woratschek, W. Sesselmann, J. Küppers, G. Ertl, H. Haberland, Phys. Rev. Lett. 55 (1985) 1231.
[34] G.K. Wertheim, D.M. Riffe, P.H. Citrin, Phys. Rev. B 49 (1994) 4834.
[35] A. Sandell, P.A. Brühwiler, A. Nilsson, P. Bennich, P. Rudolf, N. Mårtensson, Surf. Sci. 429 (1999) 309.
[36] N. Fischer, S. Schuppler, T. Fauster, W. Steinmann, Surf. Sci. 314 (1994) 89.
[37] S.Å. Lindgren, L. Walldén, Phys. Rev. B 45 (1992) 6345.
[38] H. Petek, H. Nagano, M.J. Weida, S. Ogawa, Science (1999) submitted for publication.
[39] B. Hellsing, D.V. Chakarov, L. Österlund, V.P. Zhadanov, B. Kasemo, J. Chem. Phys. 106 (1996) 982.
[40] H. Petek, H. Nagano, M.J. Weida, S. Ogawa, J. Phys. Chem. (1999) submitted for publication.

[41] M. Bauer, S. Pawlik, R. Burgermeister, M. Aeschlimann, Surf. Sci. 402–404 (1998) 62.
[42] A.G. Borisov, A.K. Kazansky, J.P. Gauyacq, Surf. Sci. 430 (1999) 165.
[43] Y.K. Kim, J. Rundgren, H. Over, in preparation.
[44] J. Osma, I. Sarría, E.V. Chulkov, J.M. Pitarke, P.M. Echenique, Phys. Rev. B 59 (1999) 10 591.
[45] X. Shi, C. Su, D. Haskett, L. Berman, C.C. Kao, M.J. Bedzyk, Phys. Rev. B 49 (1994) 14 638.
[46] B.N.J. Persson, L.H. Dubois, Phys. Rev. B 39 (1989) 8220.
[47] I.L. Shumay, U. Höfer, C. Reuß, U. Thomann, W. Wallauer, T. Fauster, Phys. Rev. B 58 (1998) 13 974.
[48] J.W. Gadzuk, Surf. Sci. 43 (1974) 44.
[49] C. Keller, M. Stichler, G. Comelli, F. Esch, S. Lizzit, D. Menzel, W. Wurth, Phys. Rev. B 57 (1998) 11 951.
[50] E.V. Chulkov, V.M. Silkin, P.M. Echenique, Phys. Rev. Lett. (1999) submitted for publication.